ELSEVIER

Contents lists available at ScienceDirect

Science of the Total Environment

journal homepage: www.elsevier.com/locate/scitotenv



Altered arsenic availability, uptake, and allocation in rice under elevated temperature



Yasmine A. Farhat ^{a,*}, Soo-Hyung Kim ^b, Angelia L. Seyfferth ^c, Long Zhang ^a, Rebecca B. Neumann ^a

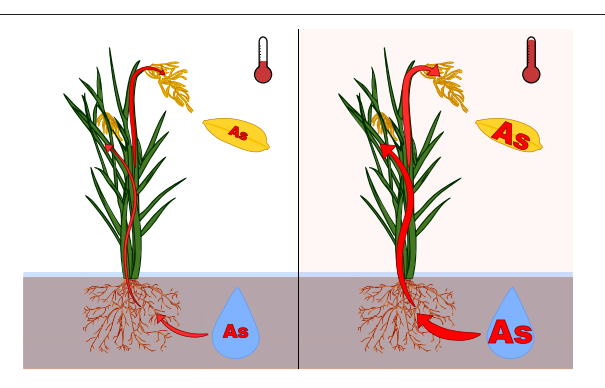
- ^a Department of Civil and Environmental Engineering, University of Washington, Seattle, WA 98195, USA
- ^b School of the Environment and Forest Sciences, University of Washington, Seattle, WA 98195, USA
- ^c Department of Plant and Soil Sciences, University of Delaware, Newark, DE 19716, USA

HIGHLIGHTS

Higher temperatures increased arsenic concentrations in all tissues, including grain.

- Temperature increased arsenic content but did not alter arsenic allocation patterns.
- At higher temperatures root plaques sorbed more arsenic per unit of iron plaque.
- Temperature-fueled mobilization of arsenic from soil was likely a key driver.

GRAPHICAL ABSTRACT



ARTICLE INFO

Article history:
Received 24 July 2020
Received in revised form 8 October 2020
Accepted 10 October 2020
Available online 17 October 2020

Editor: Charlotte Poschenrieder

Keywords: Arsenic Oryza sativa Temperature Climate change Root plaque Food quality

ABSTRACT

Climate change is expected to increase growing temperatures in rice cultivating regions worldwide. Recent research demonstrates that elevated temperature can increase arsenic concentrations in rice tissue, exacerbating an existing threat to rice quality and human health. However, the specific temperature-induced changes in the plant-soil system responsible for increased arsenic concentrations remain unclear and such knowledge is necessary to manage human dietary arsenic exposure in a warmer future. To elucidate these changes, we established four temperature treatments in climate-controlled growth chambers and grew rice plants (Oryza sativa cv. M206) in pots filled with Californian paddy soil with arsenic concentrations of 7.7 mg kg⁻¹. The four chosen temperatures mimicked IPCC forecasting for Northern California, with a roughly 2.5 °C increase between treatments (nighttime temperatures ~2 °C cooler). We observed that arsenic concentrations in porewater, root iron plaque, and plant tissue increased in response to elevated temperature. There was a positive linear relationship between temperature and rice grain arsenic, almost all of which was present as inorganic As (III). Above-ground allocation patterns were consistent across treatments. We found no upregulation in the gene encoding the OsABCC1 transporter, believed to be important for arsenic sequestration in vacuoles and thereby preventing arsenic transfer to grain. Rice plants grown at higher temperatures had more adsorbed arsenic per unit of iron plaque (measured as [As]/[Fe]), indicating temperature may impact arsenic sorption to root plaque. We present evidence that increased soil mobilization of arsenic was the driving factor responsible for increased arsenic uptake into rice grain. Transpiration, which can increase arsenic transport to roots, was also heightened with elevated temperature but appeared to play a secondary role. Our system had low soil arsenic concentrations typical for California. Our findings highlight that elevated growing temperatures may increase the risk of dietary arsenic exposure in rice systems that were previously considered low risk.

© 2020 Elsevier B.V. All rights reserved.

^{*} Corresponding author. E-mail address: yfarhat@uw.edu (Y.A. Farhat).

1. Introduction

Rice is a critical staple food for billions of people who consume rice to meet their daily caloric needs and is therefore an important component of global food security. There is an emerging appreciation that food security must consider not only food supply, but also food quality (Britz et al., 2007; DaMatta et al., 2010; Myers et al., 2014; Smith and Myers, 2018). One aspect of crop quality is the concentration of harmful elements like arsenic (As), a potent carcinogen and toxin frequently found in rice paddy environments. Rice is the major dietary source of arsenic to those without contaminated drinking water (Meharg and Zhao, 2012), and can induce genotoxic effects in humans at levels as low as 200 ng g⁻¹ (Banerjee et al., 2013). Inorganic forms of arsenic, like As(III) (i.e., arsenite) and As (V) (i.e., arsenate), are considered more toxic to humans than their common organic counter parts (Vahter and Concha, 2001) and therefore most regulatory guidelines are set to limit inorganic arsenic exposure (Codex, 2014; Food and Drug Administration FDA, 2016; European Commission, 2015).

Arsenic is highly mobile in rice paddy environments due to its geochemistry and efficient uptake by rice roots. Rice is often cultivated under flooded conditions leading to an anoxic soil environment. When soils are anoxic, solid-phase arsenic is released in a microbially mediated reductive dissolution pathway that liberates arsenic from iron (hydr)oxide minerals to which it is bound. This release occurs through dissolution of iron (hydr)oxides when Fe(III) is reduced to Fe(II), and/ or desorption of arsenic when it reduces from As(V) to As(III) (Borch et al., 2010; Cummings et al., 1999; Tufano and Fendorf, 2008; Xue et al., 2020). Solutes like arsenic travel via mass-flow and diffusion to the rhizosphere, the soil immediately surrounding and influenced by roots (Barber, 1962; Williams et al., 2014). In the rhizosphere inorganic arsenic can be intercepted by an insoluble iron plaque layer coating rice roots, primarily composed of ferrihydrite with smaller amounts of goethite and lepidocrocite (Amaral et al., 2017; Seyfferth et al., 2011; Yamaguchi et al., 2014). Arsenic species which penetrate or bypass iron plaque are taken up by root cellular transporters. As(III) is taken up by silicon transporters Lsi1 and Lsi2 (Ma et al., 2008) and As(V) is taken up by phosphate transporters (Wu et al., 2011). Arsenic concentrates in vegetative tissue within the plant and can eventually migrate toward grain. To reduce arsenic toxicity, a tonoplastic transporter, OsABCC1, shuttles inorganic arsenic into vacuoles (Song et al., 2014). Within these vacuoles, arsenic is bound to phytochelating agents and prevented from interfering with normal cellular function (Clemens and Ma, 2016). OsABCC1 expression can occur in many different tissue types and expression levels vary based on plant phenology and arsenic exposure level (Song et al., 2014).

Arsenic-relevant components of the plant-soil system are sensitive to temperature and may therefore be altered by climate change, which will increase average growing temperatures in rice growing regions worldwide (IPCC, 2013b). The magnitude of this temperature increase is uncertain, in large part because of unknown human actions to mitigate climate change. Therefore, IPCC predictions simulate various scenarios, called Representative Concentration Pathways (RCPs), which describe warming predictions from moderate to very severe. Commonly used RCPs are RCP2.6, RCP4.5, RCP6.0 and RCP8.5. During rice growing months in Northern California, an important rice cultivation region within the USA, these four scenarios predict increased average daily temperatures of up to 1.5 °C, 3 °C, 4 °C and 8 °C, respectively (IPCC, 2013a).

Increasing temperature can have numerous impacts on plant biology and function (Arai-Sanoh et al., 2010; DaMatta et al., 2010; Dieleman et al., 2012; Hatfield and Prueger, 2015). For example, it is well known that temperature stress can diminish rice spikelet fertility and overall yield (Baker, 2004; Peng et al., 2004; Porter et al., 2014; Prasad et al., 2006). There is evidence that rice yields are more susceptible to heat stress from increased nighttime temperatures than from

daytime temperatures (Kanno et al., 2009; Peng et al., 2004). These temperature-induced changes in plant biology will interact with temperature-driven arsenic mobilization (Simmler et al., 2017; Weber et al., 2010), impacting final arsenic concentrations in plant tissue and grains. Two previous studies have demonstrated that elevated temperature mobilizes soil-bound arsenic and can increase rice uptake of arsenic (Muehe et al., 2019; Neumann et al., 2017). These two studies present conflicting data as to whether an increase in temperature can directly impact concentrations of arsenic within edible grain tissue, where Muehe et al. (2019) detected this increase but Neumann et al. (2017) did not.

Here we attempt to build upon these previous studies and understand how future warming will impact the arsenic uptake pathway in rice with specific attention to three potential points for change: mobilization of arsenic from soil, transport of arsenic to roots, and allocation of arsenic within plant tissue. The mobilization rate, or the solubilization rate of arsenic from soil, is microbially meditated and can be heightened at elevated temperature when microbial rates accelerate (MacDonald et al., 1995; Weber et al., 2010). This response therefore increases the pool of dissolved arsenic (Simmler et al., 2017; Weber et al., 2010). Root uptake of arsenic may be influenced by temperature in two opposing ways. First, increased temperature can induce increased transpiration rates, leading to greater mass-flow and uptake of solutes (Lynch and St. Clair, 2004; McGrath and Lobell, 2013). Second, elevated temperature can increase iron plaque development (Neumann et al., 2017), which could suppress arsenic uptake. Arsenic distribution within the plant is influenced by both biomass gain and biomass allocation (ex. root to shoot ratio). Growth temperature impacts biomass gain in a nonlinear manner, where biomass production and spikelet fertility increase until an optimal temperature and then fall off precipitously (Arnold et al., 2019; Baker, 2004). For japonica rice varieties, the optimal growing temperature is around ~28 °C and spikelet sterility occurs between 32 and 36 °C (Baker, 2004). Arsenic allocation is also affected by its sequestration into vacuoles by OsABCC1, which prevents grain loading of arsenic (Song et al., 2014). Increased OsABCC1 expression is induced by elevated arsenic exposure and may therefore help reduce human exposure to edible arsenic.

We hypothesize that in the soil environment, elevated temperature will increase arsenic availability by boosting arsenic mobilization from soil into porewater. We also hypothesize that transport of arsenic to rice roots will increase due to greater mass-flow, but elevated temperature will simultaneously increase root plaque formation and subsequent sorption of arsenic to plaque. We anticipated that arsenic mobilization and transport will outweigh plaque sorption, resulting in increased plant uptake of arsenic with temperature. Within the plant, we hypothesize that additional arsenic uptake will trigger an upregulation of OsABCC1 expression, preventing a temperature-fueled increase in rice grain arsenic. To investigate these hypotheses, we cultivated potted rice plants using a gradient temperature approach spanning different IPCC scenarios for rice cultivating months in Northern California. We used unamended soil with a low total arsenic concentration, representative of baseline arsenic content in most rice growing soils of California.

2. Methods

2.1. Soil and plant material

2.1.1. Soil

We collected soil from a rice field in Davis, California. Total soil arsenic was $7.7\pm0.3~{\rm mg\,kg^{-1}}$ (mean \pm SD, n=3) and oxalate extractable arsenic was $73.0\pm1.8~{\rm \mug\,kg^{-1}}$ (n = 3) (Keon et al., 2001; U.S. EPA, 1996). We moistened soil with deionized water, homogenized it with a portable cement mixer, and added $21\pm1~{\rm g}$ of moistened soil into 3.8 L pots. Each chamber had 8 pots; 7 for plants and 1 as an unplanted control.

2.1.2. Germination

We grew a Californian, medium-grain rice variety, (*Oryza sativa* L. ssp. *japonica* cv. M206). We planted 10 rice seeds into moistened but not flooded soil in each pot designed for plants, and placed pots in experimental chambers to germinate for 16 days. Then we thinned seedlings to 6 per pot to match number of plants that germinated at low temperature. Treatment temperatures are further described in Section 2.2.

2.1.3. Plant care

One week after plant thinning, we flooded pots to 5 cm above soil surface and kept pots flooded with twice weekly watering. We irrigated using a $10\times$ dilution of Hoagland solution (Hoagland and Arnon, 1950). We allowed freshly prepared irrigation solution to equilibrate with chamber temperature in a carboy for at least 24 h before watering to moderate soil temperature. We recorded volume of water added to planted and unplanted pots to estimate volume of water lost by evaporation (water lost from the unplanted pot) and transpiration (planted pot water loss unplanted pot water loss). Water use efficiency was calculated by dividing mature plant biomass by volume of water transpired.

2.2. Growth chamber set-up and temperature treatments

We cultivated rice in growth chambers (DarkRoom II DR90, 36" \times 36" \times 72") at four different temperatures: 25.4 / 22.6 °C, day/night (low temperature, LT); 27.9 / 25.8 °C (medium-low, MLT); 30.5 / 28.9 °C (medium-high, MHT) and 32.9 / 31.0 °C (high temperature, HT) (Fig. 1). Temperatures were controlled using heaters (Dr Infrared Heater) and fans connected to an environmental controller (model CHHC-4i, Sentinel). Each week we used a random number generator to rearrange pots to help control for any variation in temperature throughout the chamber.

We measured air temperature at leaf level (Smart Sensor, Onset) and soil temperature at 10 cm depth in half of the pots in each treatment (TidbiT, Onset). Average light intensity at leaf level was 290 μ mol m⁻² s⁻¹ (PAR Smart Sensor, Onset). Plants grew on a 12 h light-dark schedule. Additional information about growing conditions is found in Table S1.

2.3. Sample collection

2.3.1. Timing

We defined three time points for sample collection: vegetative growth, flowering, and maturity. Briefly, we collected porewater at all three time points and collected plant and soil samples during the latter

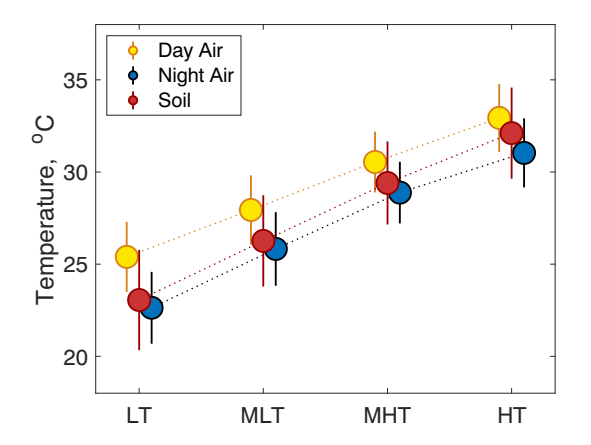


Fig. 1. Average temperatures of each treatment group over the course of the experiment with associated standard deviations. Temperature treatments are as follows: Low temperature (LT), Medium Low Temperature (MLT), Medium High Temperature (MHT), and High Temperature (HT). We measured air temperature using RH/Temperature Sensor (Onset) and soil temperature using a TidbiT Temperature Logger (Onset) buried at a 10 cm depth in 4 of 8 pots.

two time points (further described in Sections 2.3.2-2.3.3). The vegetative sampling point occurred 38 days after seeding, at the beginning of tillering stage, and was consistent across treatments. We defined flowering and maturity points observationally to adjust for differences in phenology with temperature. The flowering collection point occurred when over 75% of all plants in a given treatment had entered flowering stage. Most treatment groups flowered within the same week, with the exception of LT treatment, which flowered roughly 2 weeks later than other treatments. Maturity was defined for groups LT, MLT, and MHT by completion of grain filling. There was a roughly 2-week separation between full maturity in these three groups (first MLT, then MHT, and last LT). It was difficult to determine a full maturity time point for HT treatment because spikelets remained unfilled likely due to heat stress, even though plants were allowed to mature for longer than other treatments. Therefore, the definition of "maturity" in this treatment was not physiologically based, but rather when the treatment was harvested, which was two and a half weeks after other treatment groups.

2.3.2. Porewater collection

We collected porewater samples at vegetative, flowering, and maturity time points. We installed MicroRhizons (0.15 µm filter, Rhizosphere Research Products) into pot soil 24 h before the vegetative sampling event and left them in the pots throughout the experiment. We connected MicroRhizons to a 2-way stopcock with an attached needle used to pierce the septum of 12 mL glass vials (Exetainer, Labco). During porewater sampling events we collected three samples with vials prepared in the following ways. The first vial cleared the sampler and, because collected solution was discarded, these vials were not rigorously cleaned. Next, we collected the porewater sample for elemental analysis using an acid washed, foil wrapped, N2-purged, and evacuated vial. The last sample we collected for electrochemical characterization and carbon content, and therefore the vial was ashed as well as acid washed, foil wrapped, N2-purged, and evacuated. Each of the three vials was left to collect porewater for between 30 min and 1 h.

We preserved porewater for elemental analysis by acidifying to 2% v/v with trace metal grade HNO $_3$ immediately after opening anoxic vials. Within 2 h of collection, we transferred the sample for electrochemical characterization to an anaerobic glovebox. We removed 2 mL of each sample into a sealed vial, which we refrigerated (4 °C) for 1–2 days before analysis for dissolved organic and inorganic carbon. We measured pH and conductivity of remaining porewater solution in the glovebox.

2.3.3. Destructive harvest

We performed two destructive harvests at flowering and at maturity to collect plant and soil samples. Harvests occurred 1–2 days after porewater collection. During destructive harvests, we used a 4×30 cm cylindrical plastic tube (AMS) with a hand pressed firmly on top as a vacuum seal to collect a soil sample within the rooting zone. Immediately after removal, we capped the tube, sealed it with electrical tape, placed it in a gas impermeable liner (ESCAL, Mitsubishi Gas Chemical) with an oxygen scavenging packet (BD GasPakTM), and heat-sealed liner. We refrigerated the soil until analysis.

From each pot during both harvests, we removed two plants for physiological measurements then combined them into a composite sample for arsenic analysis, and we removed one plant for expression of *OsABCC1*. We used a random number generator to select plants. We cut the two plants at the soil surface and measured plant height, leaf number, leaf area, and tiller number. Due to high planting density, most plants did not produce tillers. Following physiological measurements, we partitioned and combined tissues from these two plants into one composite sample that was oven-dried at 60 °C (Arao et al., 2009; Li et al., 2009). During the harvest at maturity we also collected root samples from these two plants, carefully removed by hand. After removal, we rinsed roots in Milli-Q water to remove adsorbed soil and allowed roots to air-dry. For the gene-expression plant (further

described in Section 2.5), we flash froze tissue in liquid nitrogen and then stored tissue at $-80\,^{\circ}\text{C}$ until analysis.

2.4. Extractions

2.4.1. Plant tissue

We removed root plaque using a modified hot dithionite-citrate-bicarbonate (DCB) extraction (Taylor and Crowder, 1983). We cut large root systems into fragments of 0.5 g or smaller (mass known exactly) and performed extractions on all fragments of the root system. Detailed instructions of extraction procedure can be found in supplemental information. After washing, we air-dried root systems again in preparation for digestion.

We analyzed dried roots, stems, leaves, spikelets, mature hulls, and unpolished grains for arsenic content. Rice grains were separated from hulls using a simple rice huller with two rubber rollers moving in opposite directions. We ground each tissue and separated ~300 mg of sample for hot HNO3-H2O2 digestion. We then added 3 mL of H2O2 and 7.5 mL of HNO3. A microwave digester (Anton Parr) heated samples to 190 °C and digested them for 30 min. Then we decantated and brought extractant volume up to 25 or 50 mL volumetrically, based on expected arsenic concentration. Each extraction contained two sample blanks and $2/3^{\rm rds}$ of runs contained a NIST Standard Reference Material (SRM) 1568b rice flour. Average arsenic recovery from NIST 1568b was $105 \pm 12\%$ at 95% confidence limits (n=32).

We analyzed arsenic speciation in brown rice using a 2% HNO₃ extraction (Maher et al., 2013). Detailed instructions of extraction procedure can be found in supplemental information. Our extraction also contained a sample of SRM1568b rice flour sample and quantification of our detected arsenic species was within 95% confidence limits certified by supplier.

2.4.2. Soil

We air-dried collected soil in an anoxic glovebox until weight was constant. Within the glovebox we finely ground each soil sample. We subjected soil to an abbreviated two-step sequential extraction procedure. We performed extractions on soil samples collected during flowering and at maturity, for at least four pots randomly selected (via number generator) from each treatment at both time points. First, we desorbed weakly adsorbed arsenic with a concentrated phosphate extraction (Keon et al., 2001; U.S. EPA, 1996). In the second step, we removed Feassociated arsenic using a CBD extraction (Mehra and Jackson, 1958). Detailed instructions can be found in the supplemental methods.

2.5. Analytical methods

2.5.1. Elemental analysis and speciation

We used inductively coupled plasma mass spectroscopy (ICP-MS) to quantified total arsenic dissolved in porewater and in soil extractions (PerkinElmer, Elan DRC-e), and arsenic in root extractions and tissue digestions (PerkinElmer, NexION 2000, upgraded model). We analyzed porewater samples using an arsenic standard curve with a yttrium internal standard. In tissue and soil extraction analysis, we used a standard addition of arsenic to each sample to correct for stronger matrix effects. We evaluated iron removal from root plaque during DCB extraction using inductively coupled optical emission spectroscopy (ICP-OES, Perkin-Elmer, Optima 8300). We quantified inorganic As(III), As(V), DMA, and MMA in unpolished grain samples using an HPLC-ICP-MS (Thermo ICS-6000 HPLC coupled to a Thermo TQ). Separations were achieved with a PRP-X100 anion exchange column (Hamilton) with a gradient mobile phase of 3% methanol and 50 mM NaHCO₃ in 3% methanol according to established methodology (Jackson, 2015).

2.5.2. RT-qPCR

We chose to analyze flag leaf and spikelet tissue, based on their high expression during flowering stage (Song et al., 2014). We removed tissue from $-80\,^{\circ}\text{C}$ freezer and freeze-dried samples for at least 12 h. We then extracted RNA with RNeasy Plant Mini Kits (Qiagen, Valencia, CA). We used oligo (dT) 12–18 primers (Invitrogen) and M-MLV Reverse Transcriptase (Invitrogen) to produce cDNA. Finally, we preformed quantitative PCR (qPCR) of *OsABCC1* expression normalized to reference gene *HisH3*, using primer sequences published in Song et al. (2014) and SensiFASTTM SYBR® No-ROX Kits.

2.6. Statistical methods

We performed statistical analyses using MATLAB (ver. R2019a). We first analyzed temperature trends using a linear regression model fit to all data, including replicates, and plotted residuals of model output. Based on residual plots and apparent nonlinearity in many trends, we decided most outputs did not meet assumptions of a linear regression model, though there were a few exceptions. Therefore, we performed a one-way ANOVA analysis followed by Tukey HSD post-hoc using $\alpha = 0.05$. Data for ANOVA was \log_{10} transformed to reduce skew and improve normality. Data was graphed in non-transformed space for visual clarity.

2.7. Mass balance estimate of arsenic

Recognizing that both increased mobilization of arsenic into porewater and increased transpiration at higher temperatures could be involved in heightened arsenic mass-flow, we performed a simple illustrative mass balance to understand the potential arsenic response to each. Mass-flow (μg) was calculated as dissolved arsenic concentration multiplied by the amount of water transpired:

$$As_{\textit{mass}} = W \times [As]$$

where, W is the volume of water transpired per plant (L) and [As] is the dissolved arsenic concentration in the unplanted pot (μ g L $^{-1}$). At higher temperatures we expect an increase in both terms relative to LT treatment:

$$As_{mass} = (W_{LT} + \Delta W)([As]_{LT} + \Delta [As])$$

where, W_{LT} is the average volume of water transpired by LT treatment, ΔW is the increased average volume of water transpired by other three treatments relative to LT treatment, $[As]_{LT}$ is the time-averaged concentration of dissolved arsenic in the unplanted pot of LT treatment, and $\Delta[As]$ is the increase in time-averaged dissolved arsenic concentrations in other three treatments relative to LT treatment. The equation can be expanded into four terms:

$$As_{\textit{mass}} = W_{LT}[As]_{LT} + \Delta[As]W_{LT} + \Delta W[As]_{LT} + \Delta W\Delta[As]$$

The first term describes arsenic mass-flow in LT treatment, the second term describes the increase in arsenic mass-flow due solely to the temperature-fueled increase in arsenic mobilization, the third term describes the increase in arsenic mass-flow due solely to the temperature-fueled increase in transpiration, and the final term describes the increase in arsenic mass-flow due to the combined response of arsenic mobilization and transpiration to temperature (i.e. plants pulling more water with more dissolved arsenic toward their root systems at higher temperatures). It is important to note that this mass balance is an illustrative calculation of mass-flow and therefore does not account for diffusion or desorption of arsenic.

3. Results

3.1. Arsenic concentrations in rice tissue

Arsenic concentrations increased in plant tissue with temperature (Fig. 2). Statistical analysis of grain arsenic contained only 3 treatment

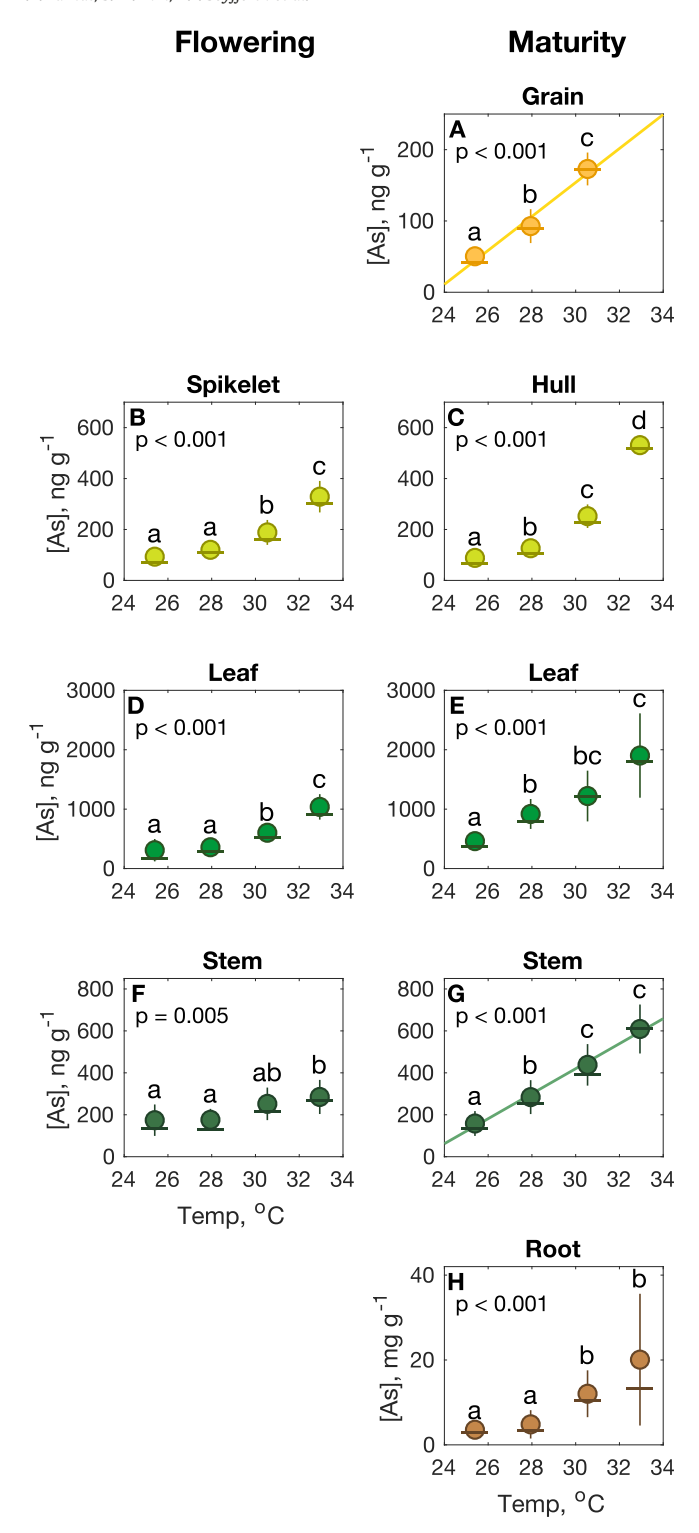


Fig. 2. Mean (circle, •) and median (dash, –) concentrations of arsenic (As) with associated interquartile ranges (error bars) vs. average daytime growing temperature during the experiment. Columns represent one of two developmental stages: flowering and maturity. No grain samples were collected from highest temperature treatment (HT) due to severe heat stress which prevented seed set. Trend lines are shown for tissues with a linear arsenic-concentration response to temperature (i.e. A and G). ANOVA *p*-value for log₁₀ transformed concentrations are shown along with statistical groups, marked with lowercase letters, determined by Tukey-Kramer post hoc at 95% confidence.

conditions (LT, MLT, and MHT) due to unfilled grain in HT that induced spikelet infertility. There was a positive linear relationship between temperature and arsenic concentration in brown rice grain as well as in stem tissue at maturity (Fig. 2A and G). In all other tissues, residuals

plots indicated that linearity or normality assumptions did not hold (Fig. S1).

Fig. 2 shows ANOVA p-values and statistical groups determined by Tukey HSD test ($\alpha=0.05$) of \log_{10} transformed data. In all tissue types the temperature impact on arsenic concentrations was highly significant (p<0.01), though not uniform across treatment groups or plant development stage. Arsenic response to temperature was weaker in tissue at flowering than in the tissues at maturity. At flowering stage, arsenic concentrations in spikelet, leaf, and stem (Fig. 2B, D, and F) were not significantly different between the two coolest temperature treatments (LT and MLT). Arsenic concentrations were increased in spikelet and leaf tissue in the MHT treatment, and in all sampled tissues, arsenic concentrations were highest in the HT treatment.

At maturity stage, the response of arsenic in plant tissue to temperature was more dramatic. In grain and hull tissue, arsenic concentrations were significantly different in each temperature treatment, with concentrations increasing across the treatment groups (Fig. 2A and C). In leaf tissue, arsenic concentrations similarly increased with temperature, though there was overlap in concentrations between MLT and MHT treatments, as well as MHT and HT treatments (Fig. 2E). Root tissue, sampled at plant maturity, showed a step response to temperature with arsenic concentrations in the two coolest treatments being significantly different than concentration in the two warmest treatments (Fig. 2H).

Almost all arsenic in grain tissue (96%) was in the arsenite, As(III), form. On average, DMA made up 3% of grain arsenic and MMA was only present above detection limits in four samples. As the vast majority of total arsenic was arsenite, ANOVA and post-hoc results shown in total grain arsenic (Fig. 2A) were mirrored in grain arsenite concentrations (Fig. S2A, p < 0.001, F = 61). There was no significant effect of temperature on grain DMA concentration (Fig. S2B, p = 0.054, F = 3.4). Sum of arsenic species was close to total grain arsenic (116 \pm 20%, mean and SD).

3.2. Arsenic content and allocation

We calculated total arsenic content (i.e., accumulation) using partitioned masses of each tissue type multiplied by relevant concentrations. A large portion of arsenic taken up by rice plants resided in roots, which contained, on average, 52% of plant arsenic (Fig. S3B). However, variance in this estimate was large (SD = 20%). Fig. 3A shows average total arsenic content in just above-ground tissue compartments and outputs of Tukey HSD post-hoc ($\alpha=0.05$). Temperature increased arsenic content of all above-ground tissue, with statistically significant differences between LT, MHT and HT treatments. Arsenic content of MLT overlapped with that of MHT for all tissue compartments, and with that of LT for stem and hull tissue.

There was a notable jump in total arsenic accumulation between MHT and HT treatments, most of which was located in leaf and stem tissue. This jump was the result of both higher arsenic concentration in these tissues (Fig. 2C and E), and an increase in vegetative tissue biomass with temperature (Fig. S4A, p < 0.001, F = 6.2). Differences in grain arsenic content were not attributable to changes in grain yield as there was no consistent decrease in yield across all treatments). Instead, there was no difference between grain biomass between LT and MLT treatment and only decrease in grain yield in MHT treatment (Fig. S4B).

Even though warmer temperatures increased arsenic accumulation, the distribution of arsenic within above-ground tissue types was similar across temperature treatments (Fig. 3B). On average 24% of above-ground arsenic was allocated to stems, 65% to leaves, and 5% to hulls. Of the three treatments which produced grain, an average of 8% of above-ground arsenic ended up in rice grains. There was no difference in percent arsenic allocated to stems, leaves, or grains across treatments (ANOVA, p > 0.05). There was a discernable statistical effect of temperature on arsenic allocated to hull (p = 0.008, F = 5.0), though the only difference was between HT and MLT.

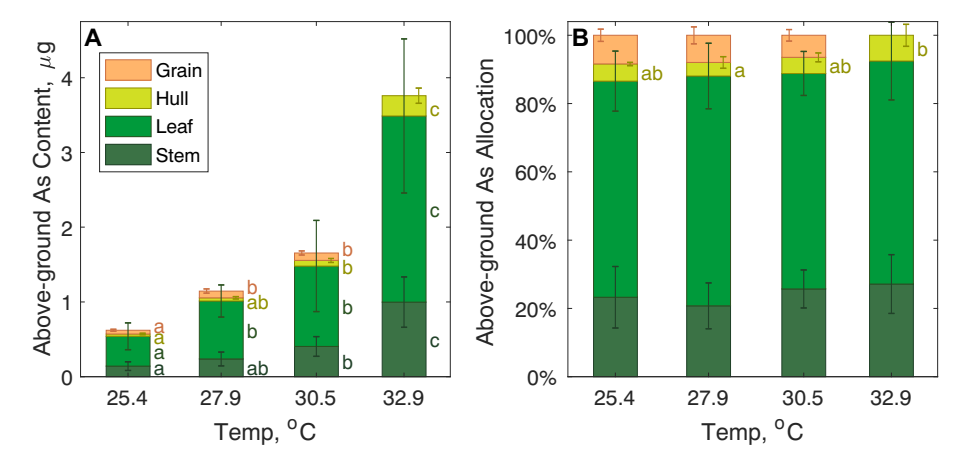


Fig. 3. (A) Average total arsenic in above-ground tissue types (grain, hull, leaf, and stem) in different temperature treatments, calculated as tissue concentration of arsenic multiplied by tissue mass. Error bars show standard deviation from mean. (B) Percentage of total above-ground arsenic present in each tissue compartment. In both graphs, lowercase letters indicate statistical differences for each tissue type based on ANOVA ($\alpha = 0.05$) performed on \log_{10} transformed values followed by Tukey-Kramer post hoc test.

To further examine potential changes in allocation, we quantified *OsABCC1* expression at flowering. We were unable to detect a consistent temperature trend in *OsABCC1* expression in response to temperature in flag leaves or spikelet (Fig. S5). There was a large degree of variance in RT-qPCR results, especially in flag leaf.

3.3. Arsenic in iron plaque

Higher temperature was associated with more sequestration of arsenic in iron plaque per gram of root biomass (Fig. 4A, p < 0.001, F = 54), where the higher two temperature treatments had more arsenic than the lower two temperature treatments. Iron plaque formation was also impacted by temperature (Fig. 4B, p < 0.001, F = 30) though the relationship was not monotonic; iron plaque, measured as mass of iron per gram of root biomass, first decreased between LT and MLT and then increased between MLT, MHT and HT treatments. The amount of arsenic sequestered per gram of iron plaque was greater in the two warmer temperature treatments than in the two cooler treatments (Fig. 4C, p < 0.001, F = 56). The increased ratio of arsenic to iron in warmer treatments indicates that the sorption capacity of iron plaque was greater in these treatments than in the cooler treatments.

3.4. Arsenic in porewater

Porewater concentrations of arsenic in planted pots were impacted by temperature at all three time points (Fig. 5). During the vegetative porewater sampling, dissolved arsenic was elevated only in HT treatment (Fig. 5A, p < 0.001, F = 81); concentrations were statistically similar across the other three temperature treatments. At both flowering and maturity stage (Fig. 5B and C, p < 0.001, F = 28 and 28), porewater arsenic concentrations in planted pots were greatest in HT, comparable in MHT and MLT, and lowest in LT. Overall, concentrations of dissolved arsenic within a given temperature treatment were greatest during the flowering stage.

At the vegetative sampling point, dissolved arsenic concentrations of the unplanted pots (n=1 per treatment) fell within interquartile range of planted pots for all treatments except HT, which had higher dissolved arsenic in the unplanted pot. At flowering and maturity time points, dissolved arsenic in the unplanted porewater was above interquartile ranges of planted pots for MHT and HT treatments. Arsenic in porewater of unplanted pots provides a visualization of arsenic concentrations without plant uptake; though we only had one pot per treatment and therefore cannot perform descriptive statistics.

Porewater dissolved iron response to temperature was less consistent. At the vegetative time point dissolved iron in porewater increased with temperature (Fig. S6A, p=0.012, F=4.33); planted pots in the HT treatment had significantly more dissolved iron than in the LT treatment, and dissolved iron in planted pots of the MHT and MLT treatments fell between these two extremes. This trend was not present in planted pots during the other two time points, though it was visible in unplanted pots (Fig. S6B and S6C). At flowering and maturity time points, dissolved iron in unplanted pots was lower than mean and median iron concentrations in planted pots for the two cooler temperature treatments, while in the two warmer temperature treatments dissolved

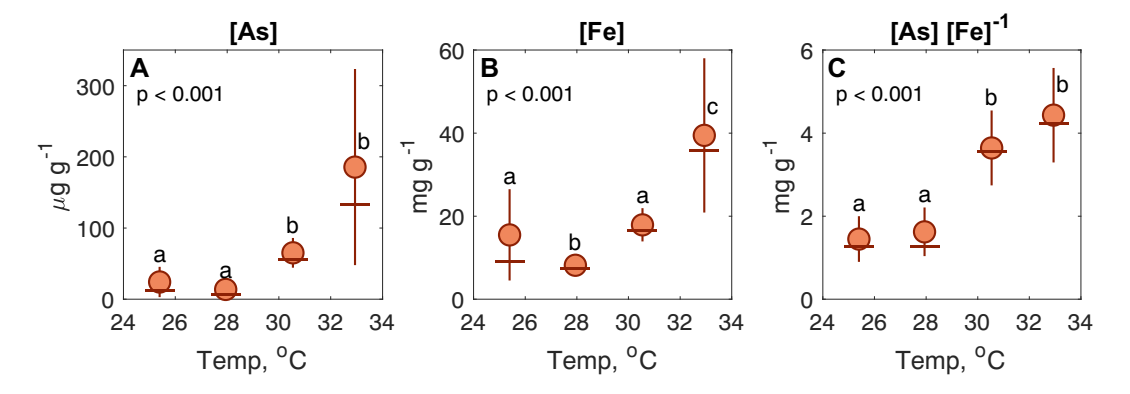


Fig. 4. Root iron plaque removed by hot dithionite-citrate-bicarbonate (DCB) extraction. (A) Arsenic, As, and (B) iron, Fe, concentrations above are the mass of both chemicals removed by extraction, normalized to root biomass. (C) As/Fe ratio is the ratio of arsenic to iron removed by DCB extraction. Means (circles, \bullet) and median (dashes, -) of each value are presented above with associated interquartile ranges (error bars). Statistical differences were determined by ANOVA ($\alpha = 0.05$) on \log_{10} transformed values followed by Tukey-Kramer post hoc, as marked by lower case letters.

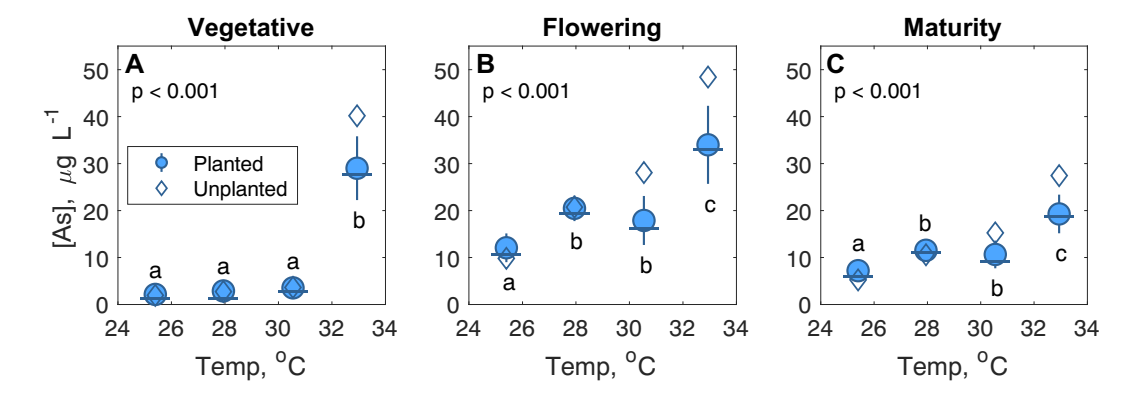


Fig. 5. Arsenic concentrations in porewater. Mean (circle, •) and median (dash, –) concentrations of arsenic (As) in eight planted pots with associated interquartile ranges (error bars). The arsenic concentration of the unplanted pot is depicted with a diamond (\Diamond). Statistical differences in dissolved arsenic concentrations in planted pots were determined by ANOVA (α = 0.05) on log₁₀ transformed values followed by Tukey-Kramer post hoc, as marked by lowercase letters.

iron in unplanted pots was greater than mean and median iron concentration in planted pots.

3.5. Arsenic in soil

There was no clear relationship between temperature and the amount of arsenic removed by either Phosphate (Phos) or CBD extraction (Fig. S7A and B). Phosphate extractable arsenic made up 72.3 \pm 8% (mean \pm SD) of extracted arsenic (arsenic removed by sequential extraction) while CBD extractable arsenic made up 28 \pm 8% of extracted arsenic (Fig. S7C and D). During the flowering time point, MHT had significantly more arsenic removed by CBD extraction relative to LT treatment during (Fig. S7A), leading to a greater relative share (%) of extracted arsenic being removed in the CBD step (Fig. S7C). However, this effect was not consistent across temperature treatments nor detectable at the harvest at maturity. Average total extracted arsenic (Phos + CBD) was within one SD of total soil arsenic (7.7 \pm 0.3 mg kg $^{-1}$, mean and SD).

3.6. Transpiration and water use efficiency

Average daily transpiration, measured as total volume of water transpired by each plant divided by number of days to maturity, and the total transpired volume of water by each plant increased with temperature (Fig. 6A and B, ANOVA, p < 0.001, F = 32 and 45). Plants in the warmer two temperature treatments transpired significantly more water and at a faster rate than those in the two cooler treatments. Water Use Efficiency (WUE) decreased with temperature (Fig. 6C, p < 0.001, F = 18), where HT WUE was significantly lower than that in the MLT and LT treatments. This difference in WUE was primarily

driven by changes in transpiration as we found no significant change in total biomass across temperature treatments groups (p=0.33, F=1.2, Fig. S4C). We note that while total biomass and above-ground biomass did not change across treatments (Fig. S4C and S4D), root biomass did experience statistical differences with temperature (Fig. S4E, p=0.015,4.1). These root biomass variations resulted in a generally decreasing root to shoot ratio with temperature (Fig. S4F, p=0.003, F=5.8); LT had the highest ratio and the two warmest treatments (MHT and HT) had the lowest ratio.

3.7. Mass balance estimate of arsenic

Our calculations (Fig. 7) indicate that average arsenic mass-flow can increase with temperature and that this increase was mainly the result of increased arsenic mobilization from soil solids (38–47%), with a lesser contribution from increased transpiration rate (2–15%). The combined effect of increased arsenic mobilization from soil and increased transpiration grew in importance across MLT, MHT and HT treatments, accounting for 3%, 26%, and 47% of arsenic mass-flow, respectively. In Fig. 7, mean observed arsenic accumulation in plants within each treatment is also shown. Accumulated arsenic includes mass of plaque-associated arsenic and mass of arsenic in plant tissues. Calculated arsenic delivery to roots via mass-flow surpassed mean observed arsenic accumulation within plants in the MLT, MHT and HT treatments.

4. Discussion

This work builds on a growing body of literature what examines arsenic concentrations in rice tissue as a function of temperature (Arao et al., 2018; Muehe et al., 2019; Neumann et al., 2017). In this

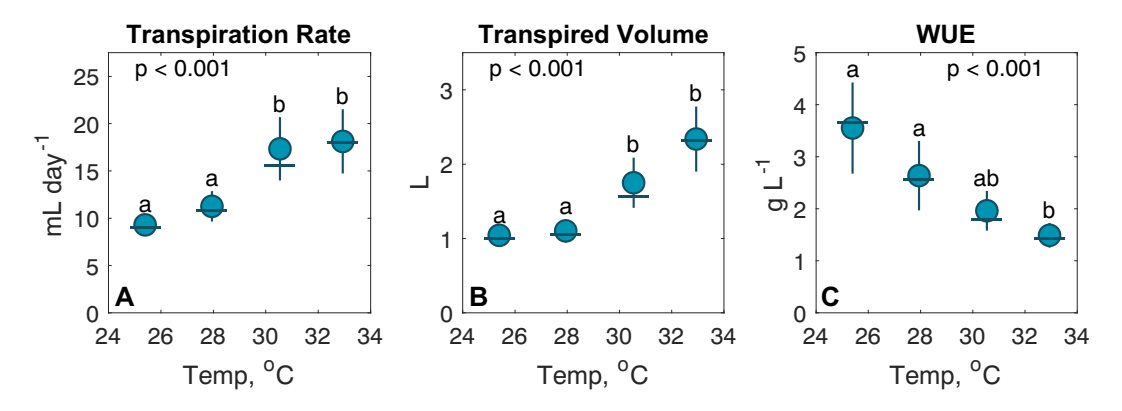


Fig. 6. Per plant water relations in (A) transpiration rate and (B) total transpired water volume with mean (circle, •), median (dash, –interquartile ranges (error bars). (C) Water use efficiency (WUE) is measured as total biomass normalized by transpiration rate. Statistical differences were determined by ANOVA ($\alpha = 0.05$) on \log_{10} transformed values followed by Tukey-Kramer post hoc, as marked by lowercase letters.

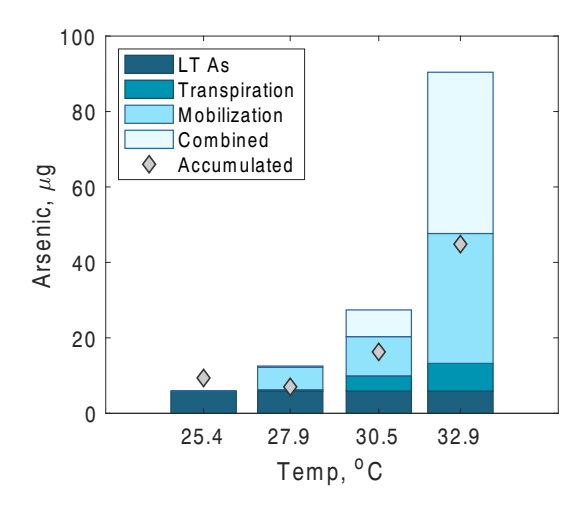


Fig. 7. Simple mass balance depicting expected increase in the mass of arsenic available for uptake or sorption to root plaque relative to low temperature treatment (LT) with amount attributable to increased mobilization of arsenic from soil, increased transpiration, and their combined effect. Diamonds (\diamondsuit) illustrate mean observed arsenic accumulation per treatment (sum of in-plant and root plaque arsenic).

experiment we sought to gain a more mechanistic understanding of how increasing temperatures impacts key components of the plantsoil system, including mobilization of arsenic from soil, transport of arsenic to rice roots, and allocation of arsenic within plant tissue.

4.1. Arsenic concentrations with temperature

We detected temperature-increased arsenic concentrations in various plant tissue types (Fig. 2). This finding is consistent with previous research showing that elevated temperature increased arsenic content in straw and leafy tissue (Muehe et al., 2019; Neumann et al., 2017). Most importantly, we observed an increasing trend between temperature and both total grain arsenic and grain inorganic arsenic (Fig. 2A, Fig. S2A), indicating that higher temperatures can increase human exposure to inorganic arsenic. This result is an important finding as previous studies have been inconsistent with regard to the ability of increased temperature to translate into higher arsenic in grain tissue. Neumann et al. (2017) was unable to track elevated temperature to increased arsenic concentration in grain using a Bangladeshi rice variety; however, Muehe et al. (2019) found an increase in grain arsenic under higher temperature conditions using the M206 variety (same variety as used in this study). Additional research is necessary to compare response rates of different rice varieties and different severity levels of arsenic contamination as these findings may inform adaptation strategies.

The system modeled here is a low arsenic system, with soil arsenic concentrations similar to average California paddy soils (Chang et al., 2004). This contamination level may help explain the sensitivity of plant tissue arsenic to temperature within our experiment, because inorganic arsenic influx exhibits a classic uptake Michaelis-Menten kinetics curve that is more linear at low concentrations but approaching an asymptotic peak at higher concentrations (Abedin et al., 2002). Neumann et al. (2017) used amended soil with a higher arsenic concentration, and uptake rates may have been closer to an asymptotic level with less sensitivity to temperature. Muehe et al. (2019) compared low and amended soil arsenic systems and found that increasing arsenic contamination of soil resulted in greater total arsenic (inorganic + organic) concentrations in rice grain. However, in their study most of the additional arsenic in rice grain was comprised of DMA, which is less toxic to humans but can cause yield declines in rice (Limmer et al., 2018a). The increased DMA may have resulted from arsenic methylating microbes responding to higher arsenic desorption in the amended soils (Dykes et al., 2020, In Press). Therefore, increased soil arsenic contamination does not necessarily lead to additional inorganic arsenic content in grains. Similar to our study, Muehe et al. (2019) found that temperature increased inorganic arsenic in grain in both the low and amended arsenic systems – indicating that temperature is an important factor in determining inorganic arsenic concentrations in grain at various levels of soil contamination.

4.2. Mobilization and soil sources

Increased microbial respiration occurs at higher temperatures and can therefore lead to heightened solubilization of arsenic (Simmler et al., 2017; Weber et al., 2010). Currently, this process is thought to be driven by increased activity of Fe(III)-reducing microorganisms and consequent reductive dissolution of As-bearing Fe(III) minerals (Weber et al., 2010). Our mass balance calculation highlighted that this temperature-driven mobilization of arsenic was a key component of increasing arsenic delivery to roots and can therefore increase arsenic accumulation in above-ground tissue (Fig. 7).

Our hypothesis that elevated temperature would increase arsenic availability in porewater was proven correct. The unplanted pot in each treatment can act as a proxy for mobilization of arsenic from soil with no arsenic loss to plant uptake; porewater concentrations in the unplanted pots showed an increase with temperature during flowering and maturity stages (Fig. 5B and C). Porewater arsenic concentrations in planted pots were not linear, though warmer temperatures did increase dissolved arsenic relative to the LT treatment (Fig. 5B and C). In the two high temperature treatments (HT and MHT) the gap between unplanted and planted dissolved arsenic was noticeable during flowering and mature stages. Such a gap likely represents the amount of arsenic lost to plant uptake, indicating that this additional pool of arsenic released at higher temperatures was taken up into plant tissue.

We used phosphate and CBD extractions to simulate arsenic pools accessible by competitive ion desorption and iron reduction, respectively (Keon et al., 2001; Mehra and Jackson, 1958). These two arsenic pools are likely assessable to soil microbes. Arsenic removed by phosphate and CBD extractions showed little change over time and between treatments (Fig. S7). Thus, there was no substantial change to these two pools of microbially accessible arsenic, supporting the claim that increased dissolved arsenic was a stronger predictor of arsenic in tissue than in solid phase arsenic. Given that soil solid phases hold a much larger amount of arsenic than the fraction found in the dissolved phase, it is not surprising that we were unable to detect reductions in arsenic content found in the soil but were able to detect changes in porewater concentrations.

4.3. Transport to roots

Plant uptake of solutes is influenced by their movement of said mineral in soil solution through the transpiration stream (Barber, 1962). It is common knowledge that increasing temperature increases vapor pressure deficit at leaf surface, increasing transpiration through stomata. We observed both increasing transpiration and decreasing seasonal water use efficiency (WUE; total biomass/water used) (Fig. 6), supporting our second hypothesis of increased arsenic mass-flow to roots. Changes in transpiration can impact uptake of solutes that travel by mass-flow and can therefore impact arsenic uptake and concentration (McGrath and Lobell, 2013; Wan et al., 2015). However, our mass balance calculation indicated increased transpiration was likely not a dominant contributor to increased arsenic uptake (Fig. 7). Transpiration was a significant factor in MHT and HT treatment when paired with increased mobilization, in "the combined effect" term. The importance of this combined effect in MHT and HT treatments is due to increasing difference in both dissolved arsenic and total transpiration relative to LT treatment (i.e. greater Δs).

One shortcoming of our mass balance calculation is that it does not include arsenic transport by diffusion, which can also be an important component of iron and arsenic delivery to roots (Williams et al.,

2014). Based on the Wilke–Chang equation (Wilke and Chang, 1955) and parameter values provided in Tanaka et al. (2013) we estimated that the molecular diffusion coefficient would only increase by ~2.5% between LT and HT treatments, while average transpiration rate increased by 95% between LT and HT treatments (Fig. 6A). Therefore, diffusion is likely less sensitive to increased temperature within this thermal range. Whether mass-flow or diffusion is the predominant mechanism of root delivery is ion specific and depends on concentration in the soil solution, soil water flow rate, and rate of root uptake of that specific ion. It is not clear exactly which is the predominant mechanism in the case of As(III) and rice, though the high physiological rates of uptake, such as those observed with arsenic and rice, tends to be associated mass-flow systems (Barber, 1962; Zhao et al., 2009).

Arsenic which travels to the rhizosphere may sorb onto iron plaque coating surrounding rice roots (Chen et al., 2005; Liu et al., 2006; Seyfferth et al., 2011; Yamaguchi et al., 2014). We found that with increasing temperature, there was greater iron plaque formation and that plaque captured more arsenic (Fig. 4A and B). As we anticipated in our hypotheses, the increased below-ground storage of arsenic was not sufficient to offset arsenic accumulation observed in above-ground plant tissue. Other work on arsenic and temperature has also shown that temperature can impact root plaque dynamics. Using XRF imaging, Neumann et al. (2017) found that rice plants grown at elevated temperatures had substantially more iron plague formation and more plagueassociated arsenic. The additional iron plaque formation at higher temperatures may be due to increased iron solubilization with temperature (Weber et al., 2010). Alternatively, Lee et al. (2013) found that arsenic addition lead to increased iron plaque formation on rice roots, though they were not able to elicit the underlying mechanism.

We also found that the [As] $[Fe]^{-1}$ ratio increased with temperature (Fig. 4C). We considered various explanations for the relationship between the [As] $[Fe]^{-1}$ ratio and temperature. One explanation is that greater arsenic delivery to roots leaded to greater arsenic incorporation in plaque during plaque formation, increasing the [As] numerator more than the [Fe] denominator. Another possible explanation for this phenomenon could be related to changes in plaque minerology and its sorption capacity for arsenic. For instance, temperature can increase root exudation rates (Bokhari and Singh, 1974; Uselman et al., 2000), and root exudates are organic ligands that can both promote the formation of ferrihydrite and prevent aging of ferrihydrite to more ordered iron forms (Cornell, 1987; Violante et al., 2003). Poorly crystalline ferrihydrite is associated with greater plaque arsenic sorption compared with more ordered iron minerals (Seyfferth et al., 2019). In either case, more extensive analysis is needed to understand the impact of elevated temperature on root plaque formation, sorption capacity, and mineral composition.

The observed average arsenic accumulation in iron plaque and plant tissue was lower than arsenic mass-flow delivery in all treatments besides LT where accumulation was slightly higher than the calculated delivery (Fig. 7). As our mass balance calculation was a fairly simple, it is not surprising that there were discrepancies between calculated and measured values. Some of these differences may be explained mechanistically. The calculated values indicate average arsenic delivered to plant roots via mass-flow. Not all of this potentially delivered arsenic necessarily sorbed to root plaque or was taken up by the plant. While arsenic uptake in rice is a highly efficient process, it is still an active process (Ma et al., 2008; Wu et al., 2011), potentially causing a discrepancy between delivery and accumulation. Other reasons for the measurement-calculation mismatch are methodological. While great care was taken in the removal of roots, tangled root networks and extremely clayey paddy soil meant that some root loss was unavoidable and therefore the true value of accumulated arsenic was likely higher than that reported. Nonetheless, this calculation provides useful insight into the potential magnitude of changes to both mobilization and transpiration, which change simultaneously with temperature.

4.4. Arsenic allocation in plants

To move toward a more mechanic understanding of arsenic response to temperature requires an analysis of not just 'how much' but also 'where' arsenic is accumulating within the plant. Arsenic concentrations in tissue decreased in the following order: root > leaf > stem > hull > grain (Fig. 2). In terms of arsenic content this sequence was the same except that grain > hull, due to greater biomass in grain relative to hull (Fig. 3A). The sensitivity of tissue arsenic (i.e., strength of the response) to temperature occurred in a similar sequence, where the increase in average leaf arsenic at higher temperatures was greater than the increase in grain arsenic at higher temperatures. This trend was also demonstrated in Neumann et al. (2017) and shows that temperature responses can be tissue specific and that increased grain arsenic is only a small fraction of the increase in total arsenic uptake (Fig. 3B).

The assessment of total arsenic found in above-ground tissue showed that more total arsenic was present in shoot tissue under elevated temperature, even when controlling for plant biomass (Fig. 3A). This result highlights that increased arsenic concentrations shown in Fig. 2 were not simply result of reduced plant biomass under heat stress. We saw no change in total above-ground biomass though we did observe an increase in stem and leaf biomass in the HT treatment relative to the other treatments, which may have slightly diluted arsenic in these tissues (Fig. S4A). There was a shift toward less root biomass and decreased root to shoot ratio at higher temperatures (Fig. S4E and S4F), which was previously observed in a Japanese rice cultivar as well (Arai-Sanoh et al., 2010). In our study, reduced root to shoot ratios did not suppress uptake to a sufficient degree to mitigate the effects of increased above-ground arsenic at elevated temperature.

The only tissue where arsenic allocation was affected by temperature was hull tissue, where percent of arsenic allocated was higher in HT relative to MLT (Fig. 3B). The larger average allocation of arsenic to hull in HT treatment was likely related to the absence of rice grain. The HT treatment had a day/night temperature of 32.9/31.0 °C. Baker (2004) found a similar temperature threshold for grain production in japonica rice, between 32 and 36 °C when plants were grown at a constant heat, or 35/31 °C day/night. In contrast, Muehe et al. (2019) did not have sterility issues in their high temperature treatment, which had a markedly higher daytime temperature but much cooler nighttime temperature (38/22 °C day/night). We posit that the heat treatment applied at night in our study conducted with the same rice variety of Muehe et al. (2019) was responsible for inducing spikelet sterility in the HT treatment. Previous research has supported the idea that rice physiological responses are more sensitive to nighttime temperatures (Kanno et al., 2009; Peng et al., 2004). This sensitivity may be relevant to future conditions, as nighttime temperatures are expected to increase more than daytime temperatures (Alexander et al., 2006; Davy et al., 2017). High DMA exposure can also induce straighthead disease in rice (Limmer et al., 2018b). However, we did not detect a statistically significant increase in grain DMA with temperature and grain DMA concentrations were quite low (Fig. S2B).

Arsenic was allocated in comparable proportions for stems and leaves across treatments (Fig. 3B), indicating that although plants were exposed to notable heat stress, this heat stress did not significantly impact arsenic flow within plant vasculature. This finding is also consistent with our inability to detect an upregulation in OsABCC1 expression across treatments, disproving our final hypothesis that OsABCC1 could mitigate arsenic allocation to grain. Song et al. (2014) characterized OsABCC1 expression in various tissue types, including roots, leaves, nodes and reproductive tissues. In our low arsenic system OsABCC1 expression may have been too low to detect significant upregulation. In short term experiments with seedlings, Song et al. (2014) was able to induce an upregulation in OsABCC1 expression in seedlings when exposed to a dramatic 375 μ g L⁻¹ shock, though not at a lower level of 37.5 μ g L⁻¹, a more similar to porewater concentration in our study. We contend that greater OsABCC1 activity should be viewed as a plant

breeding goal rather than as a mitigating factor in the face of future climate change.

4.5. Broader implications

We acknowledge that pot studies in controlled growth chambers cannot capture the full response of field grown plants to future climate conditions which will be variable across daily and inter-annual time-scales. Instead, the value of pot studies lies in allowing us to isolate and manipulate a single variable and understand its isolated impact on the rice-soil system. In this experiment we focused on the effect of temperature, one of the major threats of global climate change. Climate change will lead to increased average temperatures during rice cultivation (IPCC, 2013b) and based on our study this increased temperature will pose risks for human inorganic arsenic exposure through rice.

Relevant guidelines to reduce dietary arsenic exposure are [1] a 200 mg kg⁻¹ inorganic arsenic limit for polished white rice recommended by the FAO/WHO (Codex Alimentarius Commission, 2014) and [2] a 100 mg kg⁻¹ limit for inorganic arsenic limit in all rice used in infant food (Food and Drug Administration FDA, 2016). Average total and inorganic arsenic concentrations in Californian rice are 170 mg kg⁻¹ and 130 mg kg⁻¹ respectively (California's Office of Environmental Health Hazard and Assessment OEHHA, 2017); some of the lowest concentrations in rice grown around the world (Consumer Reports, 2012). The rice system represented in this study was not excessively contaminated and therefore arsenic concentrations of rice grain in the LT treatment were well below these safety standards recommended for infants. Raising the average growth temperature by roughly 5 °C increased total and inorganic arsenic levels well beyond the safety standard used for infants - demonstrating that rice systems that have historically been considered of low concern may become less safe in a warmer future.

Our results highlight the importance of temperature driven soil mobilization in exacerbating arsenic contamination of rice. Plant physiological responses to temperature (i.e., biomass or transpiration changes) do not seem to be a dominant controlling factors for arsenic accumulation at high temperatures. Therefore, strategies to reduced arsenic contamination of rice should focus on reducing arsenic availability, such as through alternate wetting and drying while monitoring other redox-sensitive contaminants (Carrijo et al., 2018; Honma et al., 2016; Limmer et al., 2018a), or by selecting low arsenic accumulating rice varieties (Chi et al., 2018).

CRediT authorship contribution statement

Yasmine A. Farhat: Investigation, Formal analysis, Writing - original draft, Visualization. Soo-Hyung Kim: Conceptualization, Methodology, Writing - review & editing, Funding acquisition. Angelia L. Seyfferth: Resources, Writing - review & editing. Long Zhang: Methodology, Resources, Supervision. Rebecca B. Neumann: Conceptualization, Methodology, Writing - review & editing, Funding acquisition.

Declaration of competing interest

The authors declare that they have no known competing financial interests or personal relationships that could have appeared to influence the work reported in this paper.

Acknowledgements

We would like to thank the numerous undergraduate researchers at the University of Washington who helped with the completion of this work, including Mikaela Balkind, Olivia Hargrave, Catherine Ikeda, Colin Kolbus, Evan Lester, Alex Ratcliff and Teresa Wang. Thanks, as well to Stuart Strand for access to equipment and technical knowledge on qPCR, to Hyungmin "Tony" Rho for guidance on rice plant cultivation,

and to Matt Limmer for training on arsenic speciation procedures. This publication is based upon work supported by the University of Washington Innovation Award, a grant from the National Science Foundation (1740042), and the National Science Foundation Graduate Research Fellowship (1762114). Any opinion, findings, conclusions or recommendations expressed in this material are those of the authors and do not necessarily reflect the views of the National Science Foundation.

Appendix A. Supplementary data

Supplementary data to this article can be found online at https://doi.org/10.1016/j.scitotenv.2020.143049.

References

- Abedin, M.J., Feldmann, J., Meharg, A.A., 2002. Uptake kinetics of arsenic species in rice plants. Plant Physiol. 128, 1120–1128.
- Alexander, L.V., Zhang, X., Peterson, T.C., Caesar, J., Gleason, B., Klein Tank, A.M.G., et al., 2006. Global observed changes in daily climate extremes of temperature and precipitation. J. Geophys. Res. 111.
- Amaral, D.C., Lopes, G., Guilherme, L.R.G., Seyfferth, A.L., 2017. A new approach to sampling intact Fe plaque reveals Si-induced changes in Fe mineral composition and shoot as in rice. Environ. Sci. Technol. 51, 38–45.
- Arai-Sanoh, Y., Ishimaru, T., Ohsumi, A., Kondo, M., 2010. Effects of soil temperature on growth and root function in rice. Plant Prod. Sci. 13, 235–242.
- Arao, T., Kawasaki, A., Baba, K., Mori, S., Matsumoto, S., 2009. Effects of water management on cadmium and arsenic accumulation and dimethylarsinic acid concentrations in Japanese rice. Environ. Sci. Technol. 43, 9361–9367.
- Arao, T., Makino, T., Kawasaki, A., Akahane, I., Kiho, N., 2018. Effect of air temperature after heading of rice on the arsenic concentration of grain. Soil Sci. Plant Nutr. 64, 433–437.
- Arnold, P.A., Kruuk, L.E.B., Nicotra, A.B., 2019. How to analyse plant phenotypic plasticity in response to a changing climate. New Phytol. 222, 1235–1241.
- Baker, J.T., 2004. Yield responses of southern US rice cultivars to CO₂ and temperature. Agric. For. Meteorol. 122, 129–137.
- Banerjee, M., Banerjee, N., Bhattacharjee, P., Mondal, D., Lythgoe, P.R., Martinez, M., et al., 2013. High arsenic in rice is associated with elevated genotoxic effects in humans. Sci. Rep. 3, 2195.
- Barber, S.A., 1962. A diffusion and mass-flow concept of soil nutrient availability. Soil Sci. 93, 39–49.
- Bokhari, U.G., Singh, J.S., 1974. Effects of temperature and clipping on growth, carbohydrate reserves, and root exudation of western wheatgrass in hydroponic culture. Crop Sci. 14, 790–794.
- Borch, T., Kretzschmar, R., Kappler, A., Cappellen, P.V., Ginder-Vogel, M., Voegelin, A., et al., 2010. Biogeochemical redox processes and their impact on contaminant dynamics. Environ. Sci. Technol. 44, 15–23.
- Britz, S.J., Prasad, P.V.V., Moreau, R.A., Allen, L.H., Kremer, D.F., Boote, K.J., 2007. Influence of growth temperature on the amounts of tocopherols, tocotrienols, and γ -oryzanol in brown rice. J. Agric. Food Chem. 55, 7559–7565.
- California's Office of Environmental Health Hazard and Assessment [OEHHA], 2017. Naturally occurring concentrations of listed chemicals in unprocessed foods; inorganic arsenic in white and brown rice. Title 27, California Code of Regulations. California Environmental Protection Agency.
- Carrijo, D.R., Akbar, N., Reis, A.F.B., Li, C., Gaudin, A.C.M., Parikh, S.J., et al., 2018. Impacts of variable soil drying in alternate wetting and drying rice systems on yields, grain arsenic concentration and soil moisture dynamics. Field Crop Res. 222, 101–110.
- Chang, A.C., Page, A.L., Krage, N.J., 2004. Role of Fertilizer and Micronutrient Applications on Arsenic, Cadmium, and Lead Accumulation in California Cropland Soils. California Department of Food and Agriculture.
- Chen, Z., Zhu, Y.G., Liu, W.J., Meharg, A.A., 2005. Direct evidence showing the effect of root surface iron plaque on arsenite and arsenate uptake into rice (*Oryza sativa*) roots. New Phytol. 165, 91–97.
- Chi, Y., Li, F., Tam, NF.-y., Liu, C., Ouyang, Y., Qi, X., et al., 2018. Variations in grain cadmium and arsenic concentrations and screening for stable low-accumulating rice cultivars from multi-environment trials. Sci. Total Environ. 643, 1314–1324.
- Clemens, S., Ma, J.F., 2016. Toxic heavy metal and metalloid accumulation in crop plants and foods. Annu. Rev. Plant Biol. 67, 489–512.
- Codex Alimentarius Commission, 2014. Report of the Either Session of the Codex Committee on Contaminants in Foods. 37th Session. Joint FAO/WHO Food Standards Programme, Geneva, Switzerland.
- Consumer Reports, 2012. Arsenic in your Food: Our Findings Show a Real Need for Federal Standards for this Toxin.
- Cornell, R.M., 1987. Comparison and classification of the effects of simple ions and molecules upon the transformation of ferrihydrite into more crystalline products. Z. Pflanzenernähr. Bodenkd. 150, 304–307.
- Cummings, D.E., Caccavo, F., Fendorf, S., Rosenzweig, R.F., 1999. Arsenic mobilization by the dissimilatory Fe(III)-reducing bacterium Shewanella alga BrY. Environ. Sci. Technol. 33, 723–729.
- DaMatta, F.M., Grandis, A., Arenque, B.C., Buckeridge, M.S., 2010. Impacts of climate changes on crop physiology and food quality. Food Res. Int. 43, 1814–1823.

- Davy, R., Esau, I., Chernokulsky, A., Outten, S., Zilitinkevich, S., 2017. Diurnal asymmetry to the observed global warming. Int. J. Climatol. 37, 79–93.
- Dieleman, W.I., Vicca, S., Dijkstra, F.A., Hagedorn, F., Hovenden, M.J., Larsen, K.S., et al., 2012. Simple additive effects are rare: a quantitative review of plant biomass and soil process responses to combined manipulations of CO₂ and temperature. Glob. Chang. Biol. 18. 2681–2693.
- Dykes, G.E., Chari, N.R., Seyfferth, A.L., 2020. Si-induced DMA desorption is not the driver for enhanced DMA availability after Si addition to flooded soils. Sci. Total Environ. 739.
- European Commision, 2015. Commission Regulation (EU) 2015/1006 of 25 June 2015 amending Regulation (EC) No 1881/2006 as regards maximum levels of inorganic arsenic in foodstuffs. Off. J. Eur. Union L161, 14–16.
- Food and Drug Administration [FDA], 2016. In: Services, Us.Do.Ha.H. (Ed.), Inorganic Arsenic in Rice Cereals for Infants: Action Level Guidance for Industry Draft Guidance. Center for Food Safety and Applied Nutrition, Rockville, MD, USA.
- Hatfield, J.L., Prueger, J.H., 2015. Temperature extremes: effect on plant growth and development. Weather Clim. Extremes 10, 4–10.
- Hoagland, D.R., Arnon, D.I., 1950. The water-culture method for growing plants without soil. Circ. Calif. Agric. Exp. Station. 347 (32 pp).
- Honma, T., Ohba, H., Kaneko-Kadokura, A., Makino, T., Nakamura, K., Katou, H., 2016. Optimal soil Eh, pH, and water Management for simultaneously minimizing arsenic and cadmium concentrations in rice grains. Environ. Sci. Technol. 50, 4178–4185.
- IPCC, 2013a. Annex I: Atlas of global and regional climate projections. [van Oldenborgh, G.J., M. Collins, J. Arblaster, J.H. Christensen, J. Marotzke, S.B. Power, M. Rummukainen and T. Zhou (eds.)]. In: Stocker, T.F., Qin, D., Plattner, G.-K., Tignor, M., Allen, S.K., Boschung, J., Nauels, A., Xia, Y., Bex, V., Midgley, P.M. (Eds.), Climate Change 2013: The Physical Science Basis. Contribution of Working Group I to the Fifth Assessment Report of the Intergovernmental Panel on Climate Change. Cambridge University Press, Cambridge, United Kingdom and New York, NY, USA.
- IPCC, 2013b. Climate Change 2013: The Physical Science Basis. Contribution of Working Group I to the Fifth Assessment Report of the Intergovernmental Panel on Climate Change. Cambridge University Press, Cambridge, United Kingdom and New York, NY, USA.
- Jackson, B., 2015. Fast ion chromatography-ICP-QQQ for arsenic speciation. J. Anal. At. Spectrom. 30, 1405–1407.
- Kanno, K., Mae, T., Makino, A., 2009. High night temperature stimulates photosynthesis, biomass production and growth during the vegetative stage of rice plants. Soil Sci. Plant Nutr. 55, 124–131.
- Keon, N.E., Swartz, C.H., Brabander, D.J., Harvey, C., Hemond, H.F., 2001. Validation of an arsenic sequential extraction method for evaluating mobility in sediments. Environ. Sci. Technol. 35, 2778–2784.
- Lee, C.-H., Hsieh, Y.-C., Lin, T.-H., Lee, D.-Y., 2013. Iron plaque formation and its effect on arsenic uptake by different genotypes of paddy rice. Plant Soil 363, 231–241.
- Li, R.Y., Stroud, J.L., Ma, J.F., McGrath, S.P., Zhao, F.J., 2009. Mitigation of arsenic accumulation in rice with water management and silicon fertilization. Environ. Sci. Technol. 43, 3778–3783.
- Limmer, M.A., Mann, J., Amaral, D.C., Vargas, R., Seyfferth, A.L., 2018a. Silicon-rich amendments in rice paddies: effects on arsenic uptake and biogeochemistry. Sci. Total Environ. 624, 1360–1368.
- Limmer, M.A., Wise, P., Dykes, G.E., Seyfferth, A.L., 2018b. Silicon decreases dimethylarsinic acid concentration in rice grain and mitigates straighthead disorder. Environ. Sci. Technol. 52, 4809–4816.
- Liu, W.J., Zhu, Y.G., Hu, Y., Williams, P.N., Gault, A.G., Meharg, A.A., et al., 2006. Arsenic sequestration in iron plaque, its accumulation and speciation in mature rice plants (Oryza Sativa L.). Environ. Sci. Technol. 40, 5730–5736.
- Lynch, J.P., St. Clair, S.B., 2004. Mineral stress: the missing link in understanding how global climate change will affect plants in real world soils. Field Crop Res. 90, 101–115.
- Ma, J.F., Yamaji, N., Mitani, N., Xu, X.Y., Su, Y.H., McGrath, S.P., et al., 2008. Transporters of arsenite in rice and their role in arsenic accumulation in rice grain. Proc. Natl. Acad. Sci. 105, 9931–9935.
- MacDonald, N.W., Zak, D.R., Pregitzer, K.S., 1995. Temperature effects on kinetics of microbial respiration and net nitrogen and sulfur mineralization. Soil Sci. Soc. Am. J. 59, 233–240
- Maher, W., Foster, S., Krikowa, F., Donner, E., Lombi, E., 2013. Measurement of inorganic arsenic species in rice after nitric acid extraction by HPLC-ICPMS: verification using XANES. Environ. Sci. Technol. 47, 5821–5827.
- McGrath, J.M., Lobell, D.B., 2013. Reduction of transpiration and altered nutrient allocation contribute to nutrient decline of crops grown in elevated CO₂ concentrations. Plant Cell Environ. 36, 697–705.
- Meharg, A.A., Zhao, F.-J., 2012. Arsenic & Rice. Springer Netherlands, Dordrecht: Dordrecht.
- Mehra, O., Jackson, M., 1958. Iron oxide removal from soils and clays by a dithionitecitrate system buffered with sodium bicarbonate. Clay Clay Miner. 7, 317–327.

- Muehe, E.M., Wang, T., Kerl, C.F., Planer-Friedrich, B., Fendorf, S., 2019. Rice production threatened by coupled stresses of climate and soil arsenic. Nat. Commun. 10, 4985.
- Myers, S.S., Zanobetti, A., Kloog, I., Huybers, P., Leakey, A.D., Bloom, A.J., et al., 2014. Increasing CO₂ threatens human nutrition. Nature 510, 139–142.
- Neumann, R.B., Seyfferth, A.L., Teshera-Levye, J., Ellingson, J., 2017. Soil warming increases arsenic availability in the rice rhizosphere. Agric, Environ, Lett. 2.
- Peng, S., Huang, J., Sheehy, J.E., Laza, R.C., Visperas, R.M., Zhong, X., et al., 2004. Rice yields decline with higher night temperature from global warming. Proc. Natl. Acad. Sci. 101, 9971–9975.
- Porter, J.R., Xie, L., Challinor, A.J., Cochrane, K., Howden, S.M., Iqbal, M.M., et al., 2014. Food security and food production systems. In: Field, C.B., Barros, V.R., Dokken, D.J., Mach, K.J., Mastrandrea, M.D., Bilir, T.E., et al. (Eds.), Climate Change 2014: Impacts, Adaptation, and Vulnerability. Part A: Global and Sectoral Aspects. Contribution of Working Group II to the Fifth Assessment Report of the Intergovernmental Panel of Climate Change. Cambridge University Press, Cambridge, United Kingdom and New York, NY, USA, pp. 485–533.
- Prasad, P.V.V., Boote, K.J., Allen, L.H., Sheehy, J.E., Thomas, J.M.G., 2006. Species, ecotype and cultivar differences in spikelet fertility and harvest index of rice in response to high temperature stress. Field Crop Res. 95, 398–411.
- Seyfferth, A.L., Webb, S.M., Andrews, J.C., Fendorf, S., 2011. Defining the distribution of arsenic species and plant nutrients in rice (*Oryza sativa L*) from the root to the grain. Geochim. Cosmochim. Acta 75, 6655–6671.
- Seyfferth, A.L., Limmer, M., Wu, W., 2019. Si and water management drives changes in Fe and Mn pools that affect as cycling and uptake in rice. Soil Syst. 3.
- Simmler, M., Bommer, J., Frischknecht, S., Christl, I., Kotsev, T., Kretzschmar, R., 2017. Reductive solubilization of arsenic in a mining-impacted river floodplain: influence of soil properties and temperature. Environ. Pollut. 231, 722–731.
- Smith, M.R., Myers, S.S., 2018. Impact of anthropogenic CO₂ emissions on global human nutrition. Nat. Clim. Chang. 8, 834–839.
- Song, W.Y., Yamaki, T., Yamaji, N., Ko, D., Jung, K.H., Fujii-Kashino, M., et al., 2014. A rice ABC transporter, OsABCC1, reduces arsenic accumulation in the grain. Proc. Natl. Acad. Sci. 111, 15699–15704.
- Tanaka, M., Takahashi, Y., Yamaguchi, N., Kim, K.-W., Zheng, G., Sakamitsu, M., 2013. The difference of diffusion coefficients in water for arsenic compounds at various pH and its dominant factors implied by molecular simulations. Geochim. Cosmochim. Acta 105, 360–371.
- Taylor, G.J., Crowder, A.A., 1983. Use of the DCB technique for extraction of hydrous Iron oxides from roots of wetland plants. Am. J. Bot. 70, 1254–1257.
- Tufano, K.J., Fendorf, S., 2008. Confounding impacts of iron reduction on arsenic retention. Environ. Sci. Technol. 42, 4777–4783.
- U.S. EPA, 1996. Method 3050B: Acid Digestion of Sediments, Sludges, and Soils, Washington, DC.
- Uselman, S.M., Qualls, R.G., Thomas, R.B., 2000. Effects of increased atmospheric CO₂, temperature, and soil N availability on root exudation of dissolved organic carbon by a N-fixing tree (Robinia pseudoacacia L.). Plant Soil 222, 191–202.
- Vahter, M., Concha, G., 2001. Role of metabolism in arsenic toxicity. Pharmacol. Toxicol. 89, 1–5.
- Violante, A., Barberis, E., Pigna, M., Boero, V., 2003. Factors affecting the formation, nature, and properties of Iron precipitation products at the soil–root Interface. J. Plant Nutr. 26, 1889–1908.
- Wan, X.-M., Lei, M., Chen, T.-B., Yang, J.-X., Liu, H.-T., Chen, Y., 2015. Role of transpiration in arsenic accumulation of hyperaccumulator Pteris vittata L. Environ. Sci. Pollut. Res. 22. 16631–16639.
- Weber, F.-A., Hofacker, A.F., Voegelin, A., Kretzschmar, R., 2010. Temperature dependence and coupling of iron and arsenic reduction and release during flooding of a contaminated soil. Environ. Sci. Technol. 44, 116–122.
- Wilke, C., Chang, P., 1955. Correlation of diffusion coefficients in dilute solutions. AICHE J. 1, 264–270.
- Williams, P.N., Santner, J., Larsen, M., Lehto, N.J., Oburger, E., Wenzel, W., et al., 2014. Localized flux maxima of arsenic, lead, and iron around root apices in flooded lowland rice. Environ. Sci. Technol. 48, 8498–8506.
- Wu, Z., Ren, H., McGrath, S.P., Wu, P., Zhao, F.J., 2011. Investigating the contribution of the phosphate transport pathway to arsenic accumulation in rice. Plant Physiol. 157, 498–508
- Xue, S., Jiang, X., Wu, C., Hartley, W., Qian, Z., Luo, X., et al., 2020. Microbial driven iron reduction affects arsenic transformation and transportation in soil-rice system. Environ. Pollut. 260.
- Yamaguchi, N., Ohkura, T., Takahashi, Y., Maejima, Y., Arao, T., 2014. Arsenic distribution and speciation near rice roots influenced by iron plaques and redox conditions of the soil matrix. Environ. Sci. Technol. 48, 1549–1556.
- Zhao, F.J., Ma, J.F., Meharg, A.A., McGrath, S.P., 2009. Arsenic uptake and metabolism in plants. New Phytol. 181, 777–794.